Deformation of the Contact Line around Spherical Particles Bound at Anisotropic Fluid Interfaces.

Nesrin Şenbil[1,2], *Anthony D. Dinsmore*[1,*]

[1]*Department of Physics, Univ. of Massachusetts Amherst MA, 01003, USA.*
[2]*Department of Physics, Univ. of Fribourg, Fribourg 1700, Switzerland.*
*Email: dinsmore@physics.umass.edu

Supplemental Materials:

The measured values of z_n and the role of a possible tilt of the rod:

The inset of Fig. 1d of the main text shows z_n vs. n. The corresponding data are tabulated here:

n	z_n (mm)	Uncertainty (mm)
0	0.44	9×10^{-5}
1	0.01	1.6×10^{-4}
2	0.11	1.5×10^{-4}
3	0.006	1.4×10^{-4}
4	0.003	1.4×10^{-4}
5	0.003	1.3×10^{-4}

The plot of Fig 1d shows a slight difference between the positive and negative values of ϕ. We attribute this difference to a slight tilt of the local interface away from horizontal, owing to the sphere's position being slightly away from the center between the two razor blades. We believe that this shift causes the non-zero – but still small – value of z_1. Figure S1 shows a plot of $z(\phi)$ for another sphere at a cylindrical interface with D_0 = 0.21 mm^{-1}, for comparison to Fig. 1d of the main text (though here F_{cap} has a different value). In this case, the data are highly symmetric under $\phi \rightarrow -\phi$.

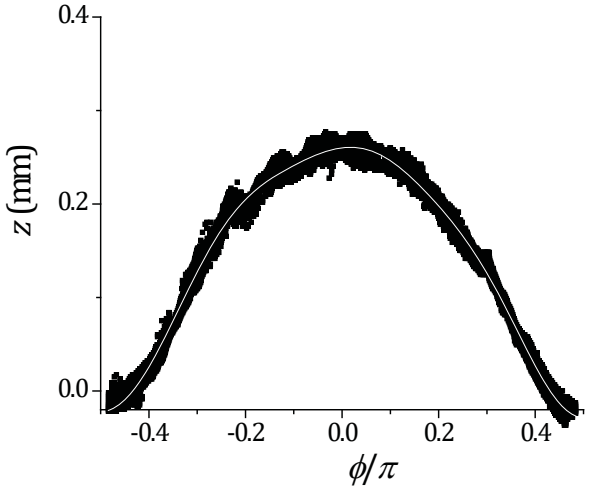

Fig S1. The height of the contact line, $z(\phi)$, measured around a sphere with D_0=0.21 mm^{-1}. The white curve shows the fit to the sum of sines and cosines as described in the main text.

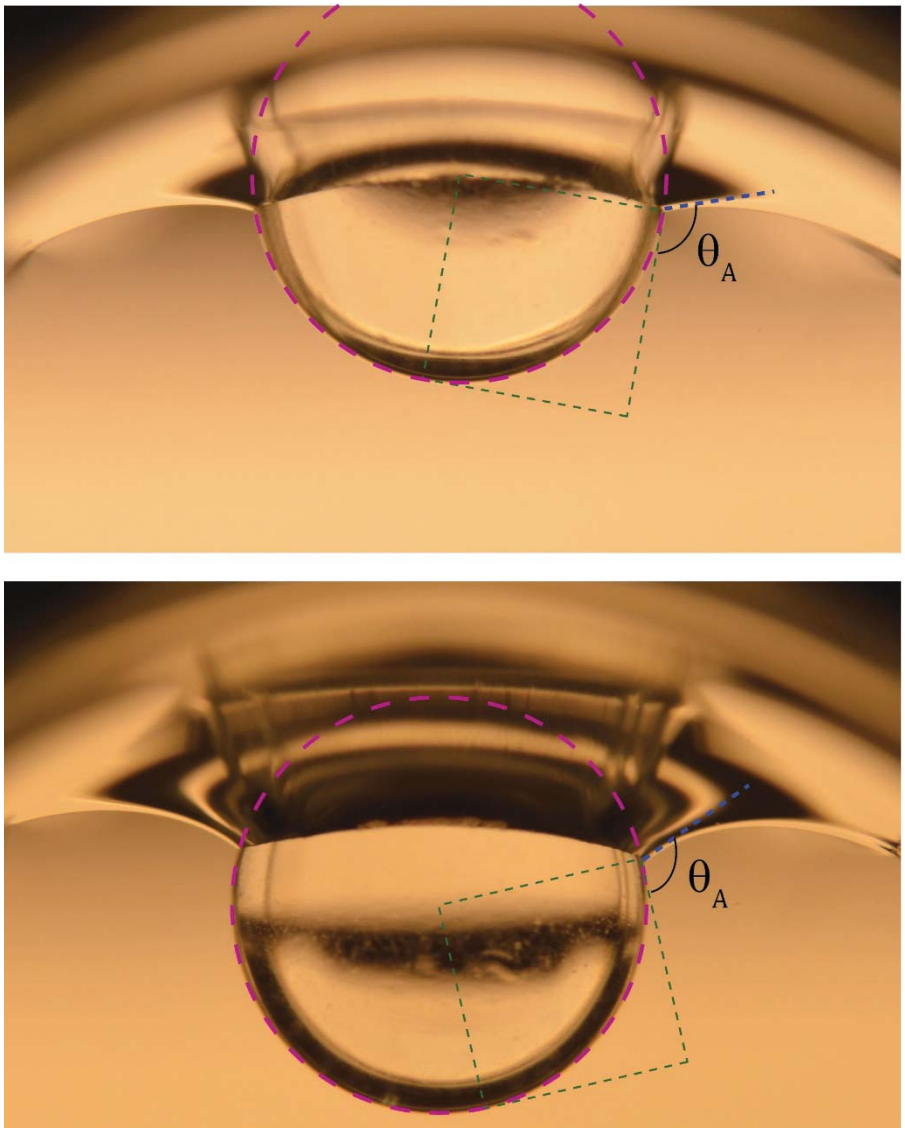

Fig. S2 Images of a sphere at two different depths within a water interface with D_0=0.21 mm^{-1}. The sphere is in the advancing limit (*i.e.*, it had been displaced downward prior to the image, so that the interface advanced across the non-wet surface of the sphere). The raw images have superimposed on them a pink circle to show the sphere's outline, a green square to show the tangent to the sphere at the contact line, and a blue dashed line to show the air-water interface near contact. The advancing contact angle, measured through the lower water phase, is indistinguishable for these two cases.

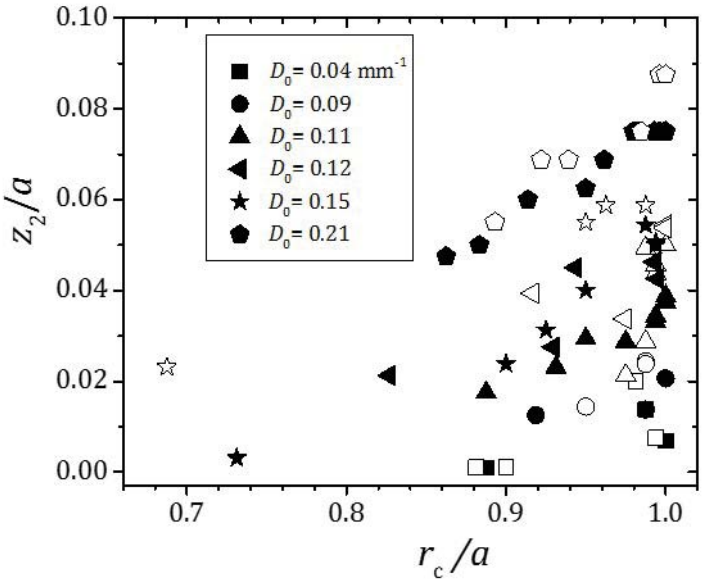

Fig. S3 A plot of z_2/a as a function of r_c/a as the immersion depth of the sphere is varied. Each plot symbol represents a series of measurements of a given sphere and an interface of given D_0. Different points correspond to different immersion depths. The filled and empty symbols represent advancing and receding contact lines, respectively. Advancing contact angles correspond to the sphere moving deeper into the water phase, so that the contact line had advanced across the non-wetted surface of the particle. In general, the value of z_2 peaks when r_c/a is close to 1 but the behavior depends on D_0. See Fig. 2 of the main text for the same data plotted as a function of $r_c^2 D_0/a$ to account for interface shape.

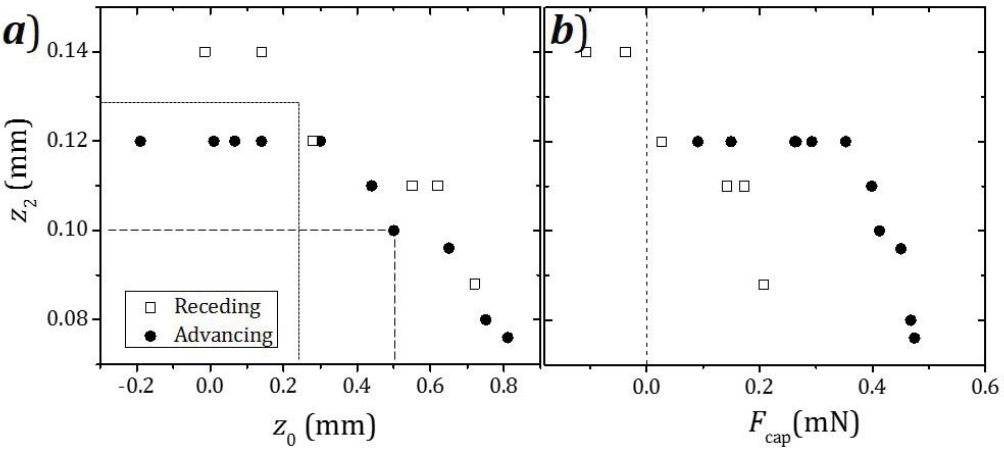

Fig. S4 Example of our methods for finding the zero-capillary-force value of the quadrupole deformation. (***a***) z_2 is plotted as a function of the mean contact-line height z_0. At a planar interface, the z_0-value corresponding to zero applied force was calculated from the measured contact angle. For the advancing and receding cases, these values are indicated by the long-dashed lines and the short-dashed lines, respectively. The zero-force deformation, z_2^0 was then extracted from the plot. In our second method (***b***), the measured z_2 is plotted *vs.* F_{cap}, which is calculated as described in the main text. The zero-force values of z_2^0 were extracted from the plot (dashed line). For the receding case, we were able to measure z_2 values at small negative and positive forces. For the advancing case, however, we were unable to see the contact line for small F_{cap} because the flat part of the fluid interface was at nearly the same level as the contact line and therefore obscured the image of the contact line.